Heterogeneous Catalysis

DOI: 10.1002/ange.200804077

Space- and Time-Resolved Combined DRIFT and Raman Spectroscopy: Monitoring Dynamic Surface and Bulk Processes during NO_x Storage Reduction

Atsushi Urakawa, Nobutaka Maeda, and Alfons Baiker*

Dedicated to the Catalysis Society of Japan on the occasion of the 50th anniversary

Various powerful in situ spectroscopic methods and their combinations have been developed to clarify and establish relations between catalytic activity and the atomic-scale environment of catalytic active sites, particularly under actual working conditions.[1] As demonstrated recently, the addition of the space-domain into typical time-domain spectroscopy allows a deeper understanding of structural effects on catalytic activity within crystals.[2] Another relevant space domain in heterogeneous catalysis is that along the axial and radial directions in a catalyst bed of a continuous fixed-bed reactor, where prominent concentration and temperature gradients are known to exist.[3] For such integral-type reactors, knowledge of concentration and temperature profiles, as well as of structural changes along the catalyst bed caused by them, is crucial for gaining insight into the governing mechanisms and for improving catalytic performance.

Herein, a time-resolved study of NO_x storage reduction is presented, with the addition of spatial resolution along the catalyst bed using combined diffuse reflectance infrared Fourier transform spectroscopy (DRIFTS) and Raman spectroscopy. The combined approach, employing a switch between DRIFTS and Raman spectroscopy within a single setup is known to yield rich chemical information.[4] In this study, simultaneous detections of the two spectroscopic methods within a single setup are achieved which give access to both surface and bulk information because of the greatly different local sensitivity of the two methods. Particular attention is given to the position-dependent dynamic surface and bulk processes along the catalyst bed, and their relation to the overall catalytic activity.

NO_x storage reduction (NSR) has garnered considerable attention, owing to its NO_x reduction capability in oxygen-rich atmospheres and its technical potential. Considerable effort has been undertaken in the elucidation of its underlying mechanism.[5] NSR utilizes periodic switching between fuel-lean (oxidative atmosphere) and fuel-rich (reductive atmosphere) conditions of engines. Generally, chemical processes occurring during the two distinct periods of NSR are summarized as follows: 1) During fuel-lean periods, NO is oxidized to NO_2 over a noble metal component, such as Pt, and stored on an alkali or alkaline-earth metal component of the catalysts, such as Ba (only Ba is mentioned hereafter), in the form of nitrates. 2) During fuel-rich periods, the stored NO_x is released and reduced to N_2 over the noble metal, and the Ba component is regenerated for NO_x storage. Several storage and reduction mechanisms have been proposed and their relevance is still a matter of active discussion. This ambiguity is, to a large extent, caused by the difficult identification of relevant species by using solely infrared[6,7] or Raman[8] spectroscopy. A variety of Ba species, such as nitrite, nitrate, carbonate, oxide, peroxide, and hydroxide, are involved in the processes occurring during lean–rich cycles, often appearing as overlapping signals. Herein, we demonstrate that the combination of both surface-sensitive (DRIFTS) and bulk-sensitive (Raman) time-resolved detection at different catalyst-bed positions is a powerful tool to facilitate deeper understanding of complex dynamic catalytic processes and reliable band assignments.

Figure 1 A shows schematically the combined DRIFTS-Raman setup configuration. The plug-flow cell design allows fast exchange of the gaseous atmosphere between lean and rich periods, and detection perpendicular to the axial direction of the catalyst bed allows gradient profiling and identification of chemical species along the bed.[9] The Pt–Ba/CeO_2 catalyst (100 mg, 1 wt% Pt and 20 wt% Ba, 6 mm in length) was placed into the cell. Infrared light and Raman excitation laser ($\lambda = 785$ nm) were focused onto the same spot of the catalyst bed through a ZnSe window. Simultaneous IR–Raman detection is possible and high-spatial resolution in the cell positioning, down to sub-micrometer levels, can be achieved. Significant spectral changes along a catalyst bed have been detected to within a less than 1 mm distance between the IR-light focal spots, in spite of the spatial averaging effects resulting from diffuse-reflectance sampling configuration.[9] Herein, we show spectra recorded at three locations of the catalyst bed for the purposes of illustration; front, middle, and back positions (0.5, 3.0, 5.5 mm from the beginning of the bed at the gas-inlet side, respectively).

Figure 1 B shows NO_x concentrations during NSR operation (lean: $NO + O_2$ atmosphere, and rich: H_2 atmosphere, both balanced by He) at 623 K. During the first 30 s under

[*] Dr. A. Urakawa, Dr. N. Maeda, Prof. Dr. A. Baiker
Institute for Chemical and Bioengineering
Department of Chemistry and Applied Biosciences, ETH Zurich
Hönggerberg, HCI, 8093 Zurich (Switzerland)
Fax: (+41) 44-632-1163
E-mail: urakawa@chem.ethz.ch
Homepage: http://www.baiker.ethz.ch

Supporting information for this article is available on the WWW under http://dx.doi.org/10.1002/anie.200804077.

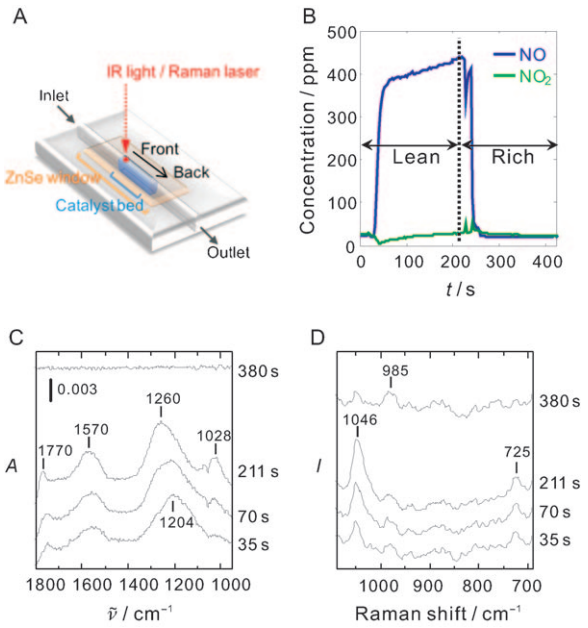

Figure 1. A) Schematic illustration of the cell, applicable to space- and time-resolved DRIFTS-Raman experiments. B) NO_x concentration; C) time-resolved DRIFT spectra; D) time-resolved Raman spectra. Spectra recorded at the front position of the catalyst bed during NSR (lean: $NO + O_2$ atmosphere; rich: H_2 atmosphere, both balanced by He) at 623 K.

fuel-lean conditions, nearly complete storage of NO_x was detected. Afterwards the storage rate dropped, although approximately 90% storage of incoming gaseous NO_x was still evident. Very little NO_2 was detected in the effluent gas during lean periods, thus indicating that all the NO_2, formed over Pt sites, was successfully captured by Ba species and/or the CeO_2 surface. After switching to fuel-rich conditions, the NO concentration decreased rapidly, followed by a sharp rise in the concentration of NO, which can be attributed to the desorption of adsorbed and/or stored NO_x, likely caused by preferential adsorption of H_2O.[10] NO_x was reduced selectively to nitrogen and no NH_3 was detected at 623 K.

Figure 1C and D show selected DRIFT and Raman spectra during the NSR process, recorded at the front position on the catalyst bed. During lean periods, the DRIFT spectra (Figure 1C) show a fast uptake of NO_x, resulting in a broad band at 1204 cm^{-1} after 35 s. This maximum shifts finally to 1260 cm^{-1} at 211 s. The shift likely results from the transformation of nitrites to nitrates by Ba species or CeO_2. Notably, the vibrational frequency of the nitrates is significantly lower than the typically reported values (1320–1430 cm^{-1})[7] of surface and ionic nitrates, although it is close to the reported values of nitrates adsorbed on CeO_2-based materials.[11] The presence of nitrate species is indicated in the DRIFT spectra by surface (1028 and 1570 cm^{-1}) and ionic (1770 cm^{-1}) nitrate bands, for which the intensity increases during lean periods. The Raman spectra (Figure 1D) clearly confirm the presence of $Ba(NO_3)_2$ (at 1046 and 725 cm^{-1}) and the absence of $Ba(NO_2)_2$ in the bulk solid, thus revealing that the nitrites are merely surface species. The low frequency of nitrate bands detected by DRIFTS is likely due to a strong interaction between the CeO_2 and Ba components, which can influence drastically the structure of the Ba component, especially at the interfaces. During rich periods, all the bands in the IR spectra described above disappeared (Figure 1C, 380 s), indicating the regeneration of the catalyst for NO_x storage. The Raman spectra, conversely, clearly show the generation of a band at 985 cm^{-1}, which is assigned to bulk $Ba(OH)_2$, as evidenced by the exclusive presence of the band among Ba reference species (nitrates, nitrites, carbonates, oxide, peroxide, and hydroxide). The presence of $Ba(OH)_2$, to our knowledge, has not been confirmed so far by IR and Raman spectroscopy. $Ba(OH)_2$ formation is likely promoted by rapid H_2O generation during rich periods. The evolution of $Ba(OH)_2$ exhibited behavior antiparallel to that of $Ba(NO_3)_2$ (see later); therefore the bulk composition mainly changes between these two components during NSR when H_2 is used as the reducing agent.

The temporal evolution of DRIFT and Raman spectra during NSR at the three catalyst-bed locations are shown in Figure 2A–F. Remarkable spectral differences were observed for the different positions along the catalyst bed. The formation of nitrites and nitrates were significantly delayed and the band intensities decreased considerably, moving from the front to the back position. In the DRIFT spectra (Figure 2A–C), the most striking difference during lean periods, besides the band intensities, is the formation of nitrites, which was detected immediately at the front position, but delayed by 70 and 120 s at the middle and back positions, respectively. Conversely, nitrates were formed from the beginning of lean periods, independently of the bed position, because of more complete NO oxidation to NO_2 over Pt towards the end of the bed (back position). The temporal profiles of surface nitrate bands at 1028 and 1570 cm^{-1} were similar to that at 1260 cm^{-1}, while the band position of bulk ionic nitrate, visible at the front position (Figure 2A), gradually shifted from 1750 to 1770 cm^{-1} during lean periods. The band at 1750 cm^{-1} is not due to bulk $Ba(NO_2)_2$, as confirmed by Raman spectroscopy, but rather caused by the formation of bulk nitrates. The chemical changes, which occur during the NO_x storage process, are likely accompanied by gradual structural reordering, that is, changes in the crystallinity of the solid during nitrate penetration from the surface into the bulk of Ba components. Furthermore, during rich periods, a remarkable difference in the reduction behaviors of nitrites and nitrates was detected. Nitrites were first reduced or desorbed from the surface and then the reduction of nitrates followed, as clearly indicated by a significant delay of the corresponding signals at the middle and back positions. The aforementioned large amount of NO, released from the catalyst at the beginning of rich periods (Figure 1B), is likely related to the disappearance of surface nitrites, thus suggesting decomposition of the nitrites and consequent release of NO into the gas phase. Moreover, the Raman spectra (Figure 2D–F) clearly indicate the difference in the amount of formed bulk $Ba(NO_3)_2$. At the front position, the amount increased drastically. However, the increase was considerably less prominent towards the back position. A similar tendency is also evident in the DRIFTS spectra (Figure 2A–C), which show much less intense surface nitrite and nitrate bands

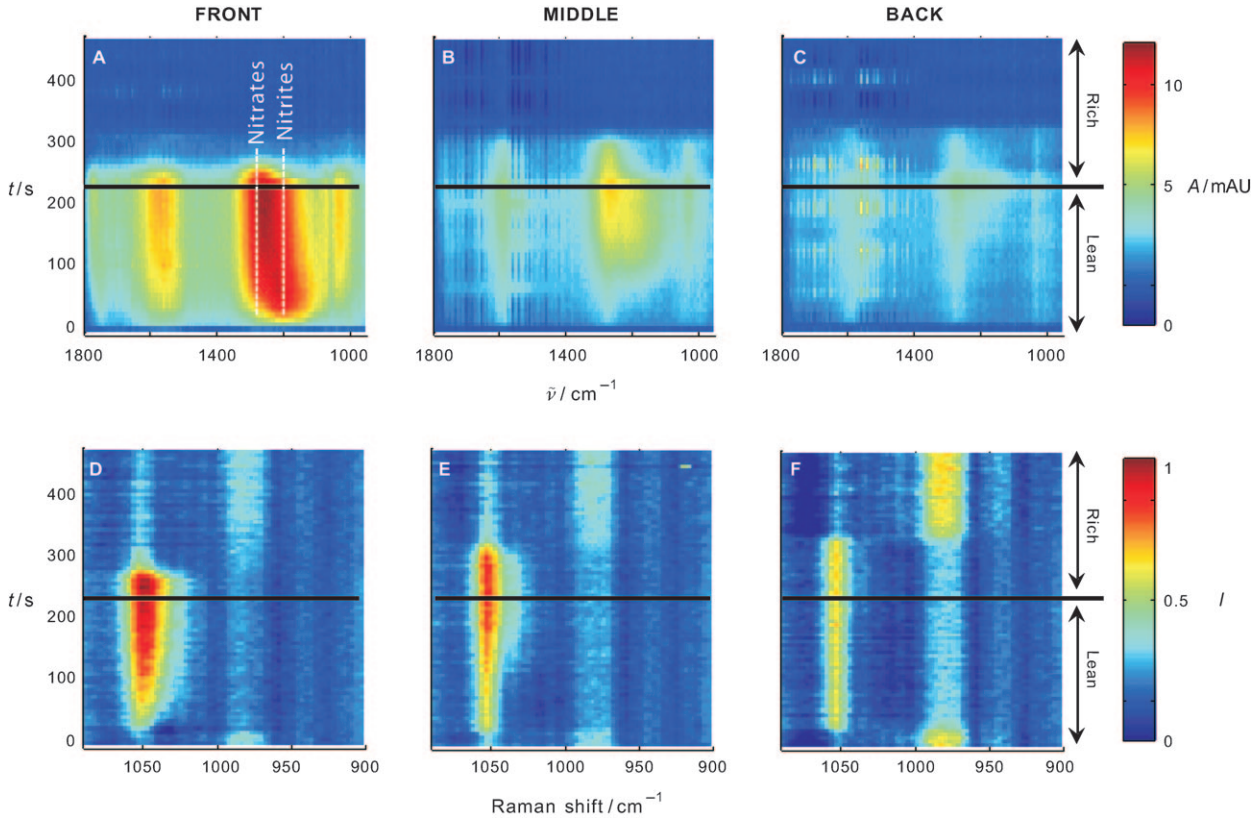

Figure 2. Time-resolved DRIFT (A–C) and Raman (D–F) spectra during NSR at the front, middle, and back positions of the catalyst bed.

towards the back position. Remarkably, 90% of the NO_x remained stored at the end of lean periods, but the majority of the NO_x was stored at the front of the catalyst bed, utilizing the bulk Ba component. The combined DRIFTS–Raman approach elucidates the position-dependent bulk utilization of the storage component, which greatly affects the efficiency of the NO_x storage process.

The frequently discussed key intermediate during NSR, NH_3, was not detected at 623 K. In the same experiment at 573 K (selected results are shown in the Supporting Information for comparison), NH_3 was released after complete reduction of N_2 and less bulk-utilization for NO_x storage was evident. Although the function of NH_3 is not discussed in detail herein, it is known to play an important role during NSR.[10,12]

An important question to address is the localized sensitivity of DRIFT and Raman spectroscopy, which depends on the properties of the investigated material, such as absorption strength, refractive index, surface roughness, and porosity, and also on the light wavelength and sampling configurations. Therefore, a quantitative answer can not be given. A rough estimate, based on comparisons between DRIFTS and other infrared spectroscopic techniques for $Ba(NO_3)_2$, demonstrated that mono- and multilayers of adsorbates, as well as bulk species below the surface, are probed equally by DRIFTS,[13] whereas no such surface species could be detected by Raman spectroscopy. As an example, the effective penetration depth into SiC changes from 50–100 nm, using a 244 nm excitation laser, to 2 mm when a 500 nm excitation laser is employed.[14] Considering the wavelength of the Raman laser used in this study ($\lambda =$ 785 nm), more bulk components are certainly probed than the surface species.

We have demonstrated a space- and time-resolved study of the dynamic surface and bulk processes occurring during NSR by combined DRIFT–Raman spectroscopy. By comparing space- and time-resolved spectra with evolved effluent gas compositions, more reliable identification and band assignments as well as a better understanding of the relevant surface and bulk processes were gained. Our next aim is to reach a firm understanding of fundamental processes on the surface and in the bulk phase during NSR, by using different supports, reducing agents, and storage components for the combined DRIFTS–Raman spectroscopic technique. Simultaneously obtained surface and bulk information, with practically relevant temporal and spatial resolution, is without doubt of great value for gaining a deeper understanding of the structure–activity relationship, and thus for the optimization of the heterogeneous catalytic process.

Experimental Section

The Pt–Ba/CeO_2 catalyst, prepared by an incipient wetness impregnation method (details are described in the Supporting Information), was placed into a newly developed reaction cell, applicable to highly space- and time-resolved measurements (ms time resolution and μm space resolution).[9] DRIFT spectra were measured with a Bruker Equinox 55 spectrometer equipped with a liquid-nitrogen-cooled

MCT detector at 4 cm^{-1} resolution. Raman spectra were obtained with an Ocean Optics QE6500 spectrometer equipped with an InPhotonics fiber optics probe and 785 nm laser excitation. The gas-phase composition was measured with a Thermostar on-line mass spectrometer (Pfeiffer Vacuum) and a ECO Physics CLD 822-S chemiluminescence detector .

The catalyst was first activated by a number of (minimum of 8) lean (0.42 vol% NO, 3.3 vol% O_2, balance He) and rich (3.3 vol% H_2, balance He) cycles, to attain steady-state (stable-response) conditions at 623 K. For each measurement, the lean–rich cycles were repeated four times, and the last three spectra were averaged to increase the signal/noise ratio. IR spectra are shown taking the last spectrum of rich periods as the background.

Received: August 18, 2008
Published online: October 30, 2008

Keywords: heterogeneous catalysis · IR spectroscopy · nitrogen oxides · Raman spectroscopy · reaction mechanisms

[1] B. M. Weckhuysen, *Phys. Chem. Chem. Phys.* **2003**, *5*, 4351 – 4360; H. Topsøe, *J. Catal.* **2003**, *216*, 155 – 164; M. A. Bañares, *Catal. Today* **2005**, *100*, 71 – 77; S. J. Tinnemans, J. G. Mesu, K. Kervinen, T. Visser, T. A. Nijhuis, A. M. Beale, D. E. Keller, A. M. J. van der Eerden, B. M. Weckhuysen, *Catal. Today* **2006**, *113*, 3 – 15.

[2] M. B. J. Roeffaers, B. F. Sels, H. Uji-i, B. Blanpain, P. L'Hoëst, P. A. Jacobs, F. C. De Schryver, J. Hofkens, D. E. De Vos, *Angew. Chem.* **2007**, *119*, 1736 – 1739; *Angew. Chem. Int. Ed.* **2007**, *46*, 1706 – 1709; M. H. F. Kox, E. Stavitski, B. M. Weckhuysen, *Angew. Chem.* **2007**, *119*, 3726 – 3729; *Angew. Chem. Int. Ed.* **2007**, *46*, 3652 – 3655; E. Stavitski, M. H. F. Kox, I. Swart, F. M. F. de Groot, B. M. Weckhuysen, *Angew. Chem.* **2008**, *120*, 3599 – 3603; *Angew. Chem. Int. Ed.* **2008**, *47*, 3543 – 3547.

[3] T. A. Nijhuis, S. J. Tinnemans, T. Visser, B. M. Weckhuysen, *Chem. Eng. Sci.* **2004**, *59*, 5487 – 5492; J. S. Choi, W. P. Partridge, C. S. Daw, *Appl. Catal. A* **2005**, *293*, 24 – 40; S. Hannemann, J. D. Grunwaldt, N. van Vegten, A. Baiker, P. Boye, C. G. Schroer, *Catal. Today* **2007**, *126*, 54 – 63.

[4] G. Le Bourdon, F. Adar, M. Moreau, S. Morel, J. Reffner, A. S. Mamede, C. Dujardin, E. Payen, *Phys. Chem. Chem. Phys.* **2003**, *5*, 4441 – 4444.

[5] N. Takahashi, H. Shinjoh, T. Iijima, T. Suzuki, K. Yamazaki, K. Yokota, H. Suzuki, N. Miyoshi, S. Matsumoto, T. Tanizawa, T. Tanaka, S. Tateishi, K. Kasahara, *Catal. Today* **1996**, *27*, 63 – 69; W. Bögner, M. Krämer, B. Krutzsch, S. Pischinger, D. Voigtländer, G. Wenninger, F. Wirbeleit, M. S. Brogan, R. J. Brisley, D. E. Webster, *Appl. Catal. B* **1995**, *7*, 153 – 171; W. S. Epling, L. E. Campbell, A. Yezerets, N. W. Currier, J. E. Parks, *Catal. Rev. Sci. Eng.* **2004**, *46*, 163 – 245.

[6] F. Prinetto, G. Ghiotti, I. Nova, L. Lietti, E. Tronconi, P. Forzatti, *J. Phys. Chem. B* **2001**, *105*, 12732 – 12745; P. Broqvist, H. Grönbeck, E. Fridell, I. Panas, *Catal. Today* **2004**, *96*, 71 – 78; A. Desikusumastuti, T. Staudt, H. Grönbeck, J. Libuda, *J. Catal.* **2008**, *255*, 127 – 133.

[7] C. Sedlmair, K. Seshan, A. Jentys, J. A. Lercher, *J. Catal.* **2003**, *214*, 308 – 316; I. Nova, L. Castoldi, L. Lietti, E. Tronconi, P. Forzatti, F. Prinetto, G. Ghiotti, *J. Catal.* **2004**, *222*, 377 – 388; Y. Su, M. D. Amiridis, *Catal. Today* **2004**, *96*, 31 – 41; A. Desikusumastuti, M. Happel, K. Dumbuya, T. Staudt, M. Laurin, J. M. Gottfried, H. P. Steinrück, J. Libuda, *J. Phys. Chem. C* **2008**, *112*, 6477 – 6486.

[8] D. Uy, K. A. Wiegand, A. E. O'Neill, M. A. Dearth, W. H. Weber, *J. Phys. Chem. B* **2002**, *106*, 387 – 394; D. Uy, A. E. O'Neill, J. Li, W. L. H. Watkins, *Catal. Lett.* **2004**, *95*, 191 – 201.

[9] A. Urakawa, A. Baiker, unpublished results.

[10] S. S. Mulla, S. S. Chaugule, A. Yezerets, N. W. Currier, W. N. Delgass, F. H. Ribeiro, *Catal. Today* **2008**, *136*, 136 – 145.

[11] M. O. Symalla, A. Drochner, H. Vogel, S. Philipp, U. Göbel, W. Müller, *Top. Catal.* **2007**, *42–43*, 199 – 202.

[12] L. Lietti, I. Nova, P. Forzatti, *J. Catal.* **2008**, *257*, 270 – 282.

[13] E. Roedel, A. Urakawa, S. Kureti, A. Baiker, *Phys. Chem. Chem. Phys.* **2008**, *10*, 6190 – 6198.

[14] H. Harima, *Microelectron. Eng.* **2006**, *83*, 126 – 129.

